frontiers | Frontiers in Earth Science

TYPE Original Research
PUBLISHED 08 September 2022
DOI 10.3389/feart.2022.970264

OPEN ACCESS

EDITED BY
John Anthony Wolff,
Washington State University,
United States

REVIEWED BY
Jin Liu,
Center for High Pressure Science and Technology Advanced Research, China
Silvio Mollo,
Sapienza University of Rome, Italy

*CORRESPONDENCE
Craig C. Lundstrom,
lundstro@illiniois.edu

SPECIALTY SECTION
This article was submitted to Petrology, a section of the journal Frontiers in Earth Science

RECEIVED 15 June 2022
ACCEPTED 19 August 2022
PUBLISHED 08 September 2022

CITATION
Lundstrom CC, Hervig R, Fischer TP, Sivaguru M, Yin L, Zhou Z, Lin X and Grossi-Diniz R (2022), Insight into differentiation in alkalic systems: Nephelinite-carbonate-water experiments aimed at Ol Doinyo Lengai carbonatite genesis.
Front. Earth Sci. 10:970264.
doi: 10.3389/feart.2022.970264

Insight into differentiation in alkalic systems: Nephelinite-carbonate-water experiments aimed at Ol Doinyo Lengai carbonatite genesis

Craig C. Lundstrom[1]*, Rick Hervig[2], Tobias P. Fischer[3], Mayandi Sivaguru[4], Leilei Yin[5], Zhenhao Zhou[1], Xiaobao Lin[1] and Rodrigo Grossi-Diniz[1]

[1]Department of Geology, University of Illinois at Urbana Champaign, Urbana, IL, United States, [2]SESE, Arizona State University, Tempe, AZ, United States, [3]Earth and Planetary Sciences, University of New Mexico, Albuquerque, NM, United States, [4]Cytometry and Microscopy to Omics Facility, Roy J. Carver Biotechnology Center, University of Illinois at Urbana Champaign, Urbana, IL, United States, [5]Beckman Institute, University of Illinois at Urbana Champaign, Urbana, IL, United States

Ol Doinyo Lengai (ODL, Tanzania, East African Rift) is the only known volcano currently erupting carbonatite on Earth with 30 yr. cycles alternating between quiescent carbonatite effusion and explosive, compositionally-zoned silicate eruptions. We performed isothermal crystallization and thermal gradient experiments involving ODL nephelinite, Na_2CO_3 and H_2O to understand magmatic differentiation in this system using SEM-EDS x-ray analysis, x-ray tomography, SIMS and LA-ICPMS to characterize samples. Isothermal crystallization experiments document that hydrous liquids coexist with nepheline+feldspar; as peralkalinity increases, temperatures decrease. Presence of Na_2CO_3 increases the solubility of water in the liquid. Experiments placing nephelinite with H_2O+ Na_2CO_3 in a 1,000–350°C thermal gradient show that rapid reaction occurs, resulting in virtually melt-free mineral aggregates having mineral layering reflecting systematic differentiation throughout the capsule. Both types of experiments argue that a continuous interconnected melt exists over a large temperature range in alkalic magmatic systems allowing for differentiation in a reactive mush zone process. Liquid compositions change from carbonate-water bearing nephelinites at high temperature down to hydrous carbonate silicate liquids at <400°C. We propose a model for ODL eruption behavior: 1) nephelinite magmas pond and build a sill complex downward with time; 2) hydrous carbonate melts form in the mush and buoyantly rise, ultimately erupting as natrocarbonatites observed; 3) H_2O contents build up in melt at the bottom of the sill complex, eventually leading to water vapor saturation and explosive silicate eruptions. The model accounts for eruption cycling and the unusual compositional zoning of ODL silicate tephras.

KEYWORDS

CO_2 degassing, thermal gradients, carbonatites, alkalic differentiation, recurrence intervals

Introduction

Differentiation of silicate melts in the upper crust is the primary driver of the diversity of igneous rocks on Earth. Although it is well accepted that mineral-melt equilibrium as a function of decreasing temperature controls compositional evolution, how differentiation occurs remains actively debated, particularly at the lower temperature end of the process. For instance, while the observed separate differentiation sequences of silica-undersaturated systems (which evolve to syenites and phonolites) and silica-saturated systems (which evolve to rhyolites and granites) are completely explained by the presence of a thermal divide along the alkali feldspar join, the "how" of the differentiation process, whether fractional crystallization or partial melting (both involving mechanical separation) or other chemical process, is simply not known.

Moreover, while compositional evolution to form granites by extraction of a minimum melt at >700°C (e.g., Tuttle and Bowen, 1958) remains the paradigm for silica-saturated systems, recent phase equilibria experiments have challenged this view showing that quartz + feldspar saturated silicate liquids with up to 37 wt% H_2O can continue down to temperatures as low as 330°C (Lundstrom, 2016, 2020). Thus, a plane representing melts saturated in quartz + feldspar exists in the peralkaline half of the K_2O-Na_2O-Al_2O_3-SiO_2 tetrahedron (Figure 1A), providing an alternative explanation to why granites form a bull's eye distribution over the minimum melt point (Tuttle and Bowen, 1958; Lundstrom, 2016). Analogously, Hamilton and MacKenzie (1965) showed that evolved silica undersaturated rock compositions similarly form a bull's eye near the temperature minimum on the nepheline-feldspar cotectic. Could a nepheline-feldspar saturation plane similarly protrude into the peralkaline half of this tetrahedron (Figure 1A)?

To test this idea, we began work on an endmember of alkalic differentiation processes, Ol Doinyo Lengai (ODL), a stratovolcano in East Africa known for eruption of ~450°C natrocarbonatite (sodium rich carbonatite) as well as higher temperature nephelinites. Indeed, the hyper-alkalic nature of ODL results in a differentiation process unlike any other igneous system, with compositional zoning of an eruption leading to *higher* silica contents as the eruption progresses (e.g., in the hotter, less differentiated magma coming out last). Here, we provide experiments using an ODL nephelinite starting material with results which may explain this anomalous behavior. Given recent experiments as well as observed ODL eruptive products, the use of terms melt or fluid or liquid may cause confusion because a continuous compositional change in liquid can exist with no straightforward boundary. Thus, for clarity, we refer to the mostly silicate liquids above 700°C as melts but liquids of variable composition below this temperature simply as liquids. When a free volatile phase exists, we will refer to this as vapor.

The idea that differentiation in the granite system might involve low temperature silicic liquids was initiated by experiments which showed that by placing andesite +4 wt% H_2O into a 950–350°C temperature gradient for 66 days, full igneous differentiation to form granite could occur at the 400°C end of a capsule in a process termed "thermal migration" (Huang et al., 2009). Below, we provide new thermal migration experiments demonstrating that differentiation in silica-undersaturated systems can also occur to similarly low temperatures (350°C). Using isothermal crystallization experiments with peralkaline starting materials, we further show that a nepheline-feldspar saturation plane indeed exists (Figure 1A), explaining how differentiation to these low temperatures can happen. Importantly, water solubility in silica-undersaturated low temperature liquids critically depends on the presence of carbonate, meaning alkalic differentiation essentially requires magmatic CO_2. Finally, the observation that differentiation within the thermal gradient experiments occurs with hardly any observable melt may explain the apparent "stealth" nature of differentiation on Earth, consistent with the lack of any largely molten magma bodies imaged by geophysics in Earth's upper crust.

Materials and methods

Background: Plutonic-volcanic connections and contradicting geophysical observations

Understanding the relationship between plutonic and volcanic rocks has vexed Earth scientists for decades. Active debate about whether granites and rhyolites reflect similar magmatic processes and timescales rages; the relationship of alkalic volcanics to associated plutonics such as syenites is even less understood, given their lower occurrence. However, alkalic ring complexes of syenites surrounding carbonatites are ubiquitously observed, providing an important spatial connection that may bear on the volcanic-plutonic connection. A prominent ring complex in North America is Magnet Cove (Arkansas) where syenites surround a core of ijolites and carbonatites.

Earth's upper crust is a major thermal boundary layer with loss of heat ultimately controlling the extent of differentiation that magmas undergo. Magma bodies are often compositionally

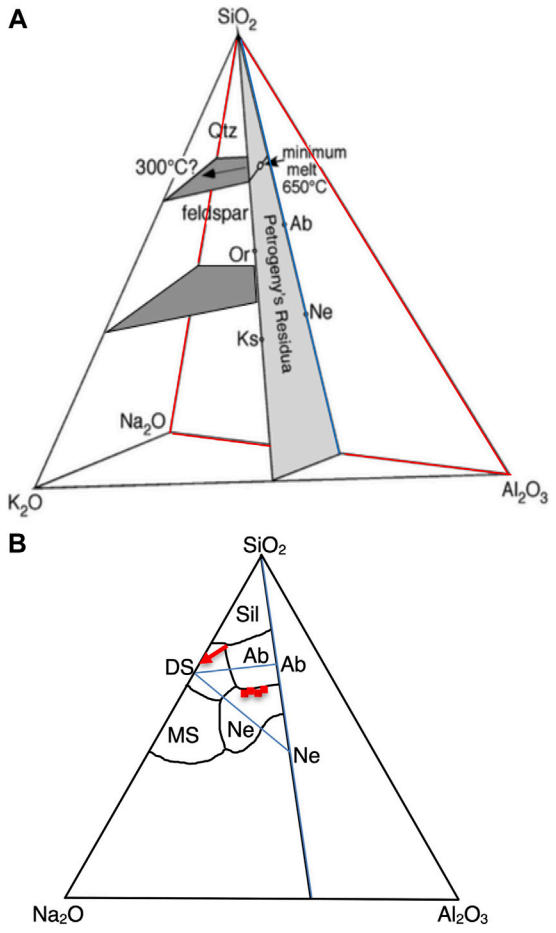

FIGURE 1
(A) Schematic phase diagram of Na_2O-K_2O-Al_2O_3-SiO_2 (+H_2O) system showing the quartz-feldspar saturated melt surface (darker gray) emanating from the minimum melt point on Petrogeny's residua (Lundstrom, 2016). A second plane of nepheline-feldspar saturated melt compositions (lower darker gray plane) should exist at lower silica. Red outlines location of ternary Na_2O-Al_2O_3-SiO_2 shown in **(B)** where the dry Na_2O-Al_2O_3-SiO_2 ternary boundaries of Schairer and Bowen (1947) have been redrawn (Sil=qtz or tridymite; Ab=albite; Ne=nepheline; MS=Na metasilicate; DS=Na disilicate). Red arrow shows continuation of Sil-Ab cotectic to Na_2O-SiO_2 join when water is added to the system. Red squares show location of four nepheline-albite saturated melts determined here; these define a line shifted slightly to lower silica relative to the nepheline-albite cotectic of Schairer and Bowen (1947). Blue triangle bounds bulk compositions of starting materials.

zoned with cooler mush existing above relatively hotter magma. Yet the fact that no large, km-scale blobs of mostly melt are seismically observed anywhere on Earth raises fundamental questions about how much liquid exists during magma differentiation. Indeed, standard models of differentiation become particularly problematic when geochronology is considered. For instance, using multiple chronometers on the same rocks, Davis et al. (2012) showed that granitic plutons undergo nearly instantaneous cooling with unresolvable age differences between U-Pb zircon closure (~800°C) to Ar-Ar in hornblende closure (~560°C) indicating that if traditional magma differentiation at >700°C actually operates, it must be extremely rapid. However, the same rocks record being held above 330°C (biotite Ar-Ar age) for up to 12 Myrs, possibly allowing low temperature differentiation (if it exists) to occur for extended durations. Several recent observations suggest that silicic magmatic systems exist in cold storage for considerable durations (Rubin et al., 2017; Ackerson et al., 2017; Ackerson et al., 2018).

The lack of visible magma bodies by seismology is curiously contradicted by newer electrical conductivity observations. For instance, extremely low electrical resistance is observed in the Cascades between Mounts Ranier, Adams and St. Helens, interpreted by Hill et al. (2009) to reflect >30% melt. Notably, this same area is very melt-poor based on seismic tomography (Lees, 1992). Combined seismology/conductivity studies may thus provide important insight into how differentiation in Earth's upper crust occurs. Such a study around ODL could be particularly useful since electrical conductivity of dry sodium carbonatite melt is >100x that of silicate melt (Gaillard et al., 2008) and water would likely increase this conductivity further. Carbonate-melt/fluids decrease dihedral angles thus increasing connectivity of fluid (Hunter and McKenzie, 1989). Low dihedral angles also mean the liquid fully wets crystal faces, which produces even greater mismatch between observed seismic velocities and electrical conductivities if hydrous carbonate liquids did indeed exist.

Background: Eruptive history and previous experiments related to ODL

Ol Doinyo Lengai is situated in the East Africa Rift in northern Tanzania. Although known for its quiescent release of natrocarbonatite at ~450°C (Dawson, 1962), ODL is actually a young stratovolcano dominantly made of nephelinites with minor phonolite generation. Cyclical volcanic activity consisting of quiescent natrocarbonatite lava effusion punctuated by explosive silicate eruptions characterizes this volcano. Explosive silicate eruptions occurred in 1933, 1965, 1983 and 2008 (Dawson et al., 1995) leading to a general cycle periodicity of ~30 years. ODL natrocarbonatite lavas are characterized by very high alkali contents and alkali/alumina ratios (e.g. >30 wt% Na_2O (Na+K)/Al>300, extreme peralkalinity; Dawson et al., 1995). Natrocarbonatite lavas also contain high contents of barium, strontium, sulfur, chlorine, phosphorous and fluorine. The nephelinite tephras are highly porphyritic containing voluminous scoriaceous lapilli with nepheline, wollastonite, combeite, Ti-andradite, apatite and clinopyroxene phenocrysts. Reynes et al. (2020) show that andradites with 11 wt% TiO_2 (like those at ODL)

have >1,000 ppm water contents, perhaps providing further evidence for the water-rich nature of ODL magmas.

The most recent eruption cycle involved natrocarbonatite lava flows from 1983 through 2007 ending with explosive eruptions in 2007–2008. Early eruptions produced tephras of dominantly nephelinite composition but with many having significant carbonatite component mixed in. During early 2008 (Jan-April), a compositionally zoned set of nephelinite tephras having little natrocarbonatite component was explosively erupted (Kervyn et al., 2010). The final tephra erupted from this sequence was carbonatite-rich nephelinite (ODL-1, last erupted tephra in Figure 2). The compositional zoning of this eruption shows the unusual nature of differentiation at ODL. Like most zoned magma systems, the coolest magma erupted first, followed by less differentiated, hotter magmas as shown by MgO increasing stratigraphically up (Figure 2). However, in behavior generally unique to ODL, the most differentiated, first-out magma was *lower* in silica than the later erupted hotter magmas. This unusual feature of ODL may provide insight into the possible processes producing compositional zoning in Earth's upper crustal systems.

The origin of carbonatites, igneous rocks that have occurred throughout Earth history, remains enigmatic and debated (Woolley and Church, 2005; Kamenetesky et al., 2021). Notably, ODL erupts natrocarbonatite while calcio- and magnesio-carbonatites, often occurring as intrusive stocks, dikes or sills, make up the majority of carbonatites in the ancient record (Jones et al., 2013). Previous experimental work has focused on assessing whether ODL natrocarbonatites form by liquid immiscibility reactions (Freestone and Hamilton, 1980; Kjarsgaard et al., 1995). While experiments have shown that two immiscible melts can form, the conjugate melt to natrocarbonatite is phonolite rather than the nephelinites that are currently co-erupted. Furthermore, the experimental conditions producing two immiscible melts are significantly higher in temperature than the eruption temperatures of ODL natrocarbonatite which are measured as 450–500°C. Previous studies have questioned the melt immiscibility interpretation based on both the phase equilibria and mismatches in trace element partitioning between immiscible melts (Nielsen and Veksler, 2002).

The finding that ODL magmas are H_2O-rich (de Moor et al., 2013) fundamentally changes the relevant phase relationships. For instance, Koster van Groos (1990) showed that a single-phase Na_2CO_3 + H_2O liquid, regardless of proportion, exists at upper crustal pressure and temperatures (400°C and 0.1 GPa), similar to those of the ODL natrocarbonatite. Furthermore, the major control on carbonate-silicate melt immiscibility depends on relative differences in structure of the two melts (Jones et al., 2013). In this light, it is not surprising that typical silicate melts and carbonatite melts remain immiscible over a wide range of P-T conditions, given differences in polymerization and viscosity and the ionic character of hydrous carbonatites. However, we note that the low temperature hydrous Na silicate liquids from Lundstrom (2020) are also unpolymerized and ionic meaning that these liquids are much more likely to be miscible with hydrous Na_2CO_3. Furthermore, based on molecular dynamics modeling, H_2O—carbonate interactions in alkalic melts are predicted to play a crucial role in stabilizing both volatile species into a single liquid, impacting both melt miscibility and degassing behaviors (Pan and Galli, 2016).

While Schairer and Bowen (1947, 1956) mapped out the Na_2O-Al_2O_3-SiO_2 system under dry conditions (Figure 1B), exploration of the peralkaline portion of this system with addition of H_2O has been minimal. In addition, examination of the silica undersaturated (nepheline-albite saturated) portion of this ternary with H_2O is nonexistent. Water bearing experiments along the nepheline-albite binary show that the eutectic drops by 234°C under water saturated conditions relative to dry conditions (Edgar, 1964). By adding a peralkaline hydrous melt, we seek to determine albite-nepheline saturated melt compositions along the cotectic valley which should continue down temperature away from the eutectic. Note that melt compositions in the silica undersaturated system will be more Al_2O_3 rich than those in the quartz saturated system. Notably work by Mysen et al. (2000) shows that increasing Al_2O_3 leads to greatly decreasing H_2O solubility. Thus, one might suspect lower H_2O solubility in these albite-nepheline saturated melts relative to the quartz albite saturated liquids of Lundstrom (2020) which had up to 37 wt% H_2O.

Methods: Isothermal crystallization experiments

The first set of experiments built off the results of Lundstrom (2020) by equilibrating a hydrous sodium disilicate starting material ($Na_2Si_2O_5$ having 33 wt% H_2O) with albite and natural nepheline crystals inside silver capsules (99.999% Ag) in cold seal vessels at 0.1 GPa. The nepheline starting material (like most natural nepheline) contains significant K_2O (~25% kalsilite). The experiments involved sealing powder mixtures (lying within the region bounded by Ab-Ne-DS; Figure 1B) at variable temperature from 3 to 21 days durations (lower temperature =longer durations).

A second set of experiments similarly reacted the hydrous sodium disilicate starting material with the natural nepheline, albite and microcline (Or_{95} amazonite from Pikes Peak, CO)+/-Na_2CO_3 at 0.1 GPa. Into one run at 630°C (5 days), two capsules were loaded—one contained just the hydrous $Na_2Si_2O_5$ powder (plus minerals) while the other contained hydrous $Na_2Si_2O_5$ with ~9 wt% Na_2CO_3. This direct comparison using two capsules was also performed at 350°C (19 days). Finally, the desire to understand a K-free system led to one experiment in which synthetic nepheline was combined with albite, hydrous Na

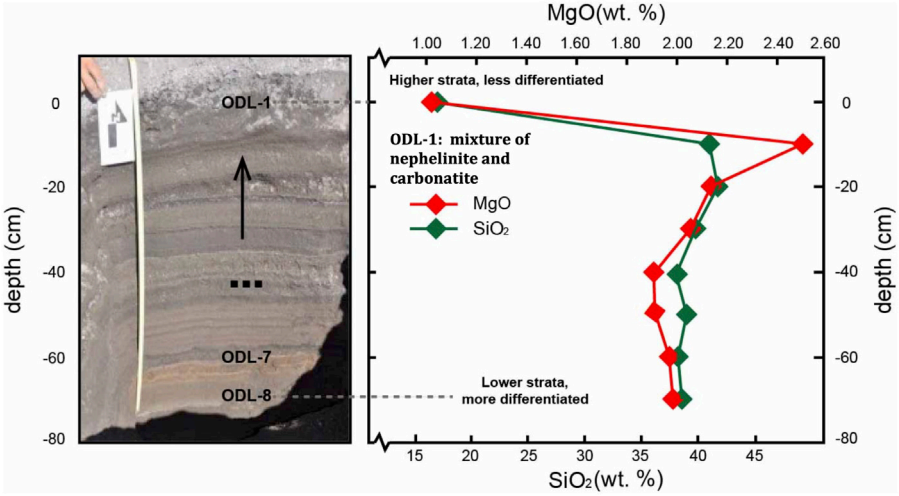

FIGURE 2
ODL zoned tephra from 2008 in stratigraphic view with compositional profile in SiO_2 and MgO. Note MgO increase up section, consistent with expectation of pre-eruption thermal zoning of magma chamber. However, unlike all other magma systems on Earth, SiO_2 increases up section (with decreasing differentiation index). ODL-1 represents a mixture of nephelinite and carbonatite, possibly consistent with it being the CO_2 rich silicate melt below the mush at the time of eruption.

disilicate and Na_2CO_3, run at 0.1 GPa and 434°C in a gold capsule for 13 days.

All experiments were rapidly quenched by dropping the bomb into water producing a quench to glass. All capsules were re-weighed after each run with experiments having mass changes outside of the 0.0002 g precision of the balance discarded. Capsules were then mounted in cold set epoxy, polished with oil and immediately loaded into the SEM for analysis to avoid problems of hydration of alkali rich glass exposed to air (Lundstrom, 2020).

Methods: Thermal gradient experiments

Three piston cylinder (Rockland Research) experiments of 1, 2, and 5 weeks duration were conducted in the experimental petrology lab at UIUC at 0.5 GPa pressure. The 2 and 5 weeks experiments both involved packing a 5% Na_2CO_3—93% ODL nephelinite powder mixture with 2% H_2O added by pipette (by mass) into a sealed 18 mm long Au-Pd_{10} capsule that sat in the imposed 1,000–350°C thermal gradient of the piston cylinder vessel. The 1 week experiment involved adding 6% $BaCO_3$ and 1% UO_2CO_3 in a layer near the capsule bottom (instead of the Na_2CO_3) along with 91% nephelinite powder with 2% H_2O added by pipette into a sealed Au-Pd_{10} capsule. The thermocouple arrangement of the piston cylinder dictates the hot end being above the cold end in the experiment, opposite to likely gradients in the Earth. However, an experiment of Lesher and Walker (1988) showed that when the cold end did occur above the hot end, the exact same thermal migration process took place—e.g., the material differentiated down temperature.

Methods: Analytical details

All experiments were characterized using multiple techniques including SEM-EDS, X-ray tomography, LA-ICPMS and SIMS. Details of analytical protocols and observations from each thermal gradient experiment are given in the appendix.

Results

Isothermal crystallization experiments

Supplementary Table S1 presents observed phases and melt compositions within the isothermal crystallization experiments. All low temperature (<500°C) runs in the first set of Ne-Ab bearing experiments (run from 819 to 330°C) were failures (not reported) due to the fact that they fell apart during grinding and polishing—all of these experiments, even those above 500°C that we report on, show vapor bubble indicating H_2O saturation (also consistent with observation of fluid emanating upon breaching the capsule).

The microcline bearing experiments, which compared two capsules run simultaneously (one with Na_2CO_3 and one

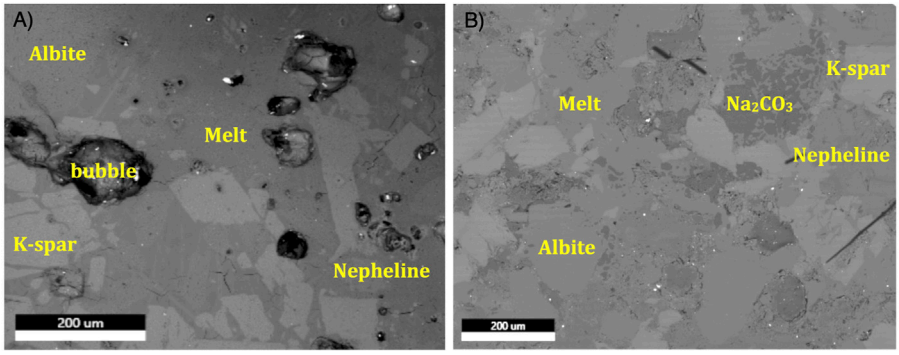

FIGURE 3
BSE images of isothermal crystallization experiments at 0.1 GPa. **(A)** Nepheline-albite-microcline-DS at 630°C; Note prominent vapor bubbles. **(B)** Nepheline-albite-microcline-DS + Na_2CO_3 at 350°C. Note the lack of vapor bubbles (DS = hydrous $Na_2Si_2O_5$).

without), allowed a clear picture of the impact of CO_2 on formation of melt and thus water solubility. This comparison results in a fundamental observation, that the presence of Na_2CO_3 changes the solubility of H_2O in the melt. Indeed, the 350°C carbonate bearing experiment produced a quench glass that shows no obvious vapor bubbles (Figure 3). The corresponding Na_2CO_3-free capsule at 350°C was puffed out (an indication of vapor saturation) and completely fell apart when opened and polished (perhaps indicating lack of melt?), making it unanalyzable. In the 630°C experiments, the carbonate-free experiment produced large vapor bubbles (like the early non-carbonate bearing H_2O-only experiments), unambiguously documenting vapor saturation. In contrast, the carbonate bearing 630°C experiment may or may not have been vapor saturated based on small amounts of porosity seen in the mount. However, clearly a much smaller volume of vapor existed in this experiment compared to the carbonate-free one. Imaging of the two carbonate-bearing experiments show that Na_2CO_3 crystals tend to disperse along the silicate grain boundaries, perhaps indicating the carbonate fluid's role in facilitating wetting of silicate crystals. Unfortunately, there were other complications in these experiments limiting their usefulness including the observation that nephelines develop large rims of a nepheline-albite solid solution (composition approximately 27 wt% Na_2O, 23 wt% Al_2O_3 and 50 wt% SiO_2). Therefore, we do not report melt compositions for the microcline bearing experiments. Finally, the sole experiment using a synthetic Na-only nepheline and Na_2CO_3 produced a nepheline-albite-melt assemblage with little evidence for a vapor phase present confirming the carbonate-H_2O effect found in the microcline experiments.

Melt compositions in the nepheline-albite experiments closely follow the phase boundaries of the dry system (Schairer and Bowen, 1947; Figure 1B). Melt compositions at higher temperature are relatively Al_2O_3 rich and become progressively more Na_2O rich down temperature while silica remains constant at ~57.5 wt%. The glass in the Na_2CO_3-saturated K-free experiment contains 17 wt% CO_2. However, considerable uncertainty exists in this composition due to difficulties of quantitation of the low energy carbon x-ray.

Water contents of the glasses are difficult to quantify but can be estimated based on observed phase proportions. For instance, 11.7 wt% H_2O was added to the K-free nepheline capsule and assuming water only enters the ~40% modal volume of the glass phase, we estimate the dissolved water content of the liquid to be ~29 wt% H_2O.

Thermal gradient experiments

In each of the 15–20 mm long capsules (ODL-1wk, ODL-2wk and ODL-5wk), we observe systematic changes in mineralogy and geochemistry as a function of position (thus temperature). Because there are essentially no visible melt pools in any of the colder, lower ¾ portions of these experiments, the only way to present compositional data is to provide bulk compositions, modal determinations and some mineral compositions—analyses of melt compositions are not possible.

Because ODL-5wk and ODL-2wk involve identical starting materials, the mineralogical changes serve to illustrate the temporal evolution of the thermal migration process. For instance, ODL-2wk quenched to a transitional nepheline+melt partially molten area near its top whereas ODL-5wk has a sharp transition between 100% melt at its top and an almost entirely crystalline lower portion. In ODL-5wk, melilite forms the liquidus phase. The shift in liquidus phase from nepheline to melilite is reproduced by IRIDIUM models (see appendix SFig. 4). Most of the observations and discussion that follow focus on experiment ODL5-wk although collectively, the three

experiments contribute to understanding the thermal gradient differentiation process.

ODL-5wk evolves to a crystal-free silicate melt in the hot, upper 25% of the capsule which abruptly shifts to a melt-poor mineralogically-layered crystal aggregate in its lower 75% (Figures 4A,B; Supplementary Table S2). Peaks in different mineral modes testify to the thorough dissolution-and-reprecipitation-based reaction process occurring as a function of temperature. As predicted by IRIDIUM, melilite occurs at highest temperature, then garnet, then clinopyroxene and finally wollastonite representing the prominent layering produced by the thermal migration process (nepheline is found throughout with little variation in its mode). A striking observation is the sharpness of layering indicated by apatite (Figure 4C) at ~400°C where a jump to 5% higher apatite mode is defined by a single line of the mineral across the capsule.

Bulk compositions of major elements in ODL-5wk follow smooth trends that reflect these changing mineral modes and the elemental contents of the phases (Supplementary Table S2; Figure 5). MgO, Al_2O_3, and even SiO_2 all decrease down temperature. Melilite compositions change in Ca#, consistent with decreasing temperature (and IRIDIUM prediction) while nepheline composition remains invariant (Supplementary Tables S3–6). Volatile element contents (SIMS spots of ~15 μm diameter) of the hot 100% melt area are homogeneous and indicate ~4 wt% CO_2 and 3 wt% H_2O. However, within the crystal-rich lower portion, these spot analyses produce highly heterogeneous CO_2 contents, reflecting randomly encountering carbonate solids along the silicate grain boundaries. F, Cl, and SO_4 analyses also vary widely, consistent with observed fluorite, halite and potassium aluminum sulfate existing at the cold end of ODL-5wk. An x-ray phase map (Figure 6) shows the interstitial material between broken silicate grains; a qualitative analysis gives 46.7 wt% Na_2O, 5.0 wt% SiO_2, 5.1 wt% S, 5.7 wt% K_2O and 37.3 wt% CaO excluding C from the analysis. Using 7 KV for C/Si analysis of this same region, we obtain ~13 wt% for CO_2. While this is only a rough composition, the finding of only these peaks (and O) is consistent with a carbonate (silicate) liquid with Na, Ca and K being the major cation components (similar to observed natrocarbonatite at ODL). Finally, the complete redistribution of U and Ba in ODL-1wk observed via x-ray tomography and SEM mapping illustrates the rapid transport process occurring leading to deposition of carbonates along the silicate phase boundaries (Supplementary Figure S6; see movie of tomography of experiment in Supplementary Material). The addition of Ba to this experiment also stabilized alkali feldspar relative to ODL-5wk and ODL-2wk.

Finally, the distribution of trace elements within ODL-5wk is very regular and clearly controlled by the major phases existing at a given location in the experiment. This is well illustrated by the distribution of each REE as a function of position (Figure 7). For instance, HREE concentrate in the location where the garnet mode peaks, reflecting their high garnet-melt partition coefficient ($^{gt/melt}D_{HREE}$) with a systematic decrease in concentration going from MREE to LREE. Correspondingly, the LREE become enriched in the bottom portion of ODL-5wk, where carbonates and apatite become most prevalent.

Discussion

Isothermal crystallization experiments, volatiles and assessment of equilibrium

The isothermal crystallization experiments show that a melt co-exists with nepheline + albite down temperature with melts becoming more peralkaline, following compositional behavior seen in the dry system (Schairer and Bowen, 1947). Addition of Na_2CO_3 appears to increase water solubility allowing a carbonate-hydrous silicate liquid to co-exist with nepheline and feldspar at 330°C.

Excepting the microcline-bearing experiments, we argue that melt compositions reported in the nepheline-feldspar crystallization experiments (Supplementary Table S1) represent a close approach to chemical equilibrium, producing changes in alumina, silica and alkali concentrations with temperature following expectation based on the dry system. The duration of experiments was similar to those of Lundstrom (2020) in which variation of starting material mixtures and time series experiments argued for attainment of equilibrium. The correspondence to the dry albite-nepheline phase boundary of Schairer and Bowen (1947) suggests consistency with previous equilibrium experiments. The high concentration of CO_2 in the peralkaline silicate liquid reflects solubility of Na_2CO_3 into these liquids as Na_2CO_3 is residual in the solid assemblage. H_2O and Na_2CO_3 appears to have mutual effects on each other's solubility suggesting a complicated structure to the liquid.

Assessing equilibrium in thermal gradient experiments must be done with the acknowledgement that compositions of phases in these experiments can only reflect transient changes occurring as components move through melt and shift the proportions of the major phases. As such, the extent to which these experiments reached the full expected redistribution of components is unknown and frankly irrelevant. However, assessments of local equilibrium can be made. In the ODL-5wk thermal gradient experiment, the systematic change in Ca# of melilite (consistent with thermodynamic prediction) and the systematic partitioning of trace elements into observed phases both argue for a relatively close approach to mineral-melt equilibrium. Close examination shows a remarkably consistent change in concentration for each REE as a function of temperature (Figure 7). Indeed, each area produces a smooth REE pattern consistent with expected patterns based on the

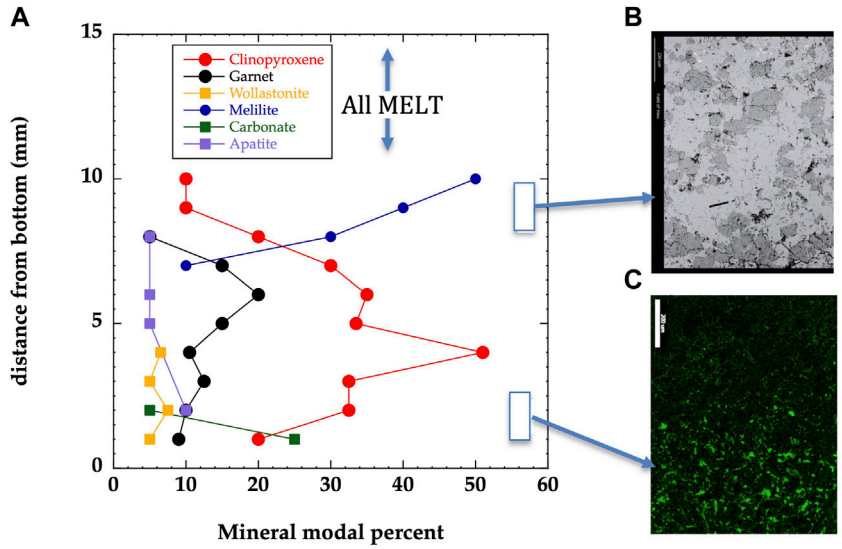

FIGURE 4
(A) ODL-5wk is modally layered as a function of temperature (position) for the Ca-rich phases: melilite mode decreases from 10 to 7 mm, the garnet mode peaks at 7 mm, the clinopyroxene mode peaks at 4 mm and finally, wollastonite is found in the bottom 3 mm. Nepheline is found throughout. **(B)** BSE image shows complete lack of melt within the crystalline assemblage just below the melt-interface (upper rectangle in A) in ODL-5wk. **(C)** X-ray map of phosphorous showing dramatic increase in apatite mode near bottom (lower rectangle in A).

mineralogy at that location. That this occurs within 5 weeks attests to extremely fast transport of elements through the liquid and, likely, a dissolution-reprecipitation dominated process for equilibrating minerals with liquid. This argument for equilibrium partitioning is further evidenced by examination of the concentration patterns with position of chemically similar element pairs (Zr-Hf or Nb-Ta; Supplementary Appendix Figure). While the shorter thermal gradient experiments may have had less time to reach equilibrium, the fact that the time series behavior, in which component migration leads to changes in liquidus phase, is consistent with thermodynamic control of the process.

Interpretation of vapor saturation in both isothermal crystallization and thermal gradient experiments is somewhat tricky. If we observe bubbles in the glass or a fluid upon opening a capsule, we have unambiguous evidence for vapor phase saturation. However, the lack of bubbles trapped in glass could be indication of the inability of low viscosity liquids to trap any vapor phase. We acknowledge this possibility but argue that lack of observation of water escaping during polishing likely argues for vapor undersaturation in the lower temperature carbonate bearing experiments. Clearly future work determining vapor saturation in mixed alkali-silicate-Na_2CO_3-H_2O systems (both silica saturated and undersaturated) is needed.

Within the thermal migration experiments, we also interpret the melt as being vapor undersaturated (in the 0.5 GPa experiments). Based on measured H_2O and CO_2 in the glass of ODL-5wk, retention of mass including volatiles within the capsule appears to have occurred, arguing for closed system behavior. While CO_2 solubility is known to strongly correlate with pressure and alkalinity (Lowenstern, 2001; Moussallam et al., 2016), the measured CO_2 concentrations in the silicate glass at the high temperature end of ODL-5wk (~4 wt% CO_2) far exceed predicted CO_2 solubility in typical silicate melts. Furthermore, previous work shows that a single-phase 80%H_2O-20%Na_2CO_3 liquid can exist at 400°C and 0.2 GPa (Koster van Groos, 1990) and our nepheline-albite experiment at 434°C produced a hydrous silicate liquid with 17 wt% CO_2. Thus, we interpret that a carbonate-water-silicate liquid occurs at the low temperature end of ODL-5wk. The presence of a H_2O-Na_2CO_3 liquid at the cold end is also consistent with molecular dynamics simulations that indicate H_2O-CO_3-alkali fluids (rather than dissolved CO_2) dominate at upper crustal pressures (Pan and Galli, 2016).

Insights into differentiation from thermal gradient experiments

At the outset, we emphasize that while thermal gradient experiments can be highly illustrative of processes of differentiation in an imposed temperature gradient, we do not advocate that Earth's magma chambers necessarily represent an analogous process of a statically held magma

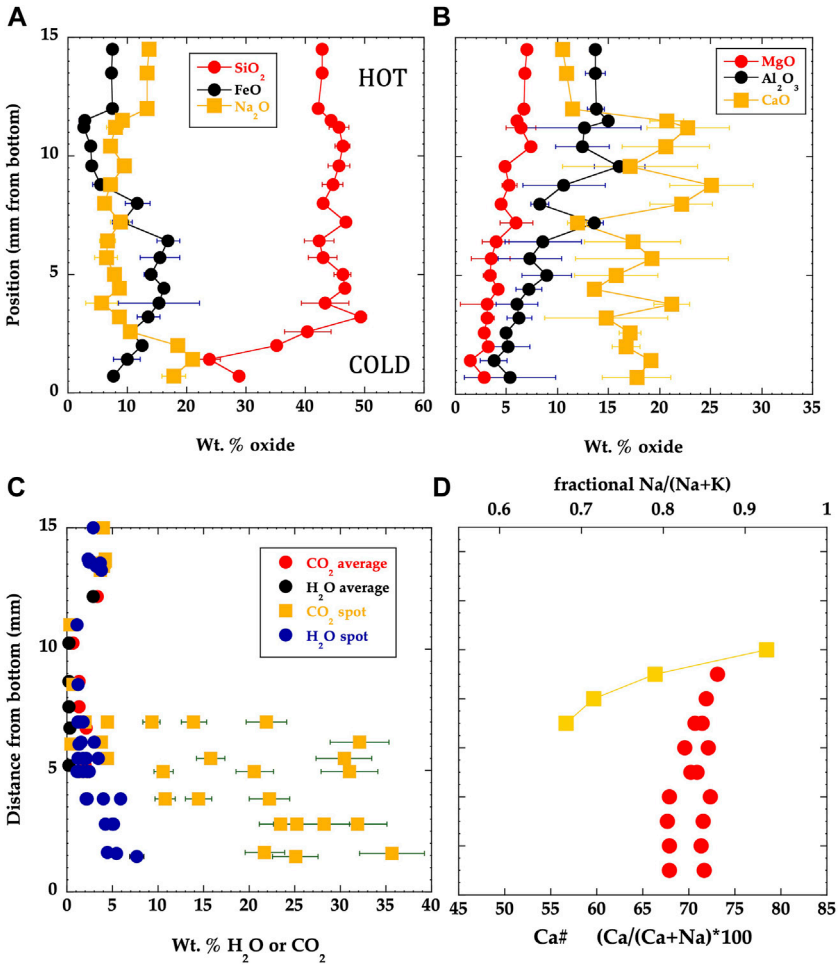

FIGURE 5
Variations in major element concentrations in experiment ODL-5wk. **(A,B)** Silica decreases toward the colder end of the charge, unlike typical magma differentiation trends on Earth but resembling differentiation at ODL. Na_2O increase and MgO and Al_2O_3 decrease down temperature as observed in most igneous differentiation. **(C)** Concentrations of H_20 and CO_2 with position in the experiment—averages represent pooling 5–10 spots in a given area of the experiment while spots represent single 15 mm diameter SIMS analysis. Homogeneous concentrations occur in the glassy hot portion but extreme heterogeneity occurs in the crystalline portion, reflecting deposition of carbonate phases along the silicate grain boundaries. Water content increases in the melt relative to the starting material, consistent with its concentrating due to formation of the anhydrous crystalline assemblage. In contrast, CO_2 concentration in the melt is lower than the starting material, reflecting carbonate migrating to form carbonate solids within the colder crystalline portion. **(D)** Melilite Ca# decreases down temperature while the Na/(Na+K) of nepheline remains invariant throughout the capsule.

body in an imposed gradient over longer spatial and temporal scales—a more dynamic process clearly must exist to overcome diffusion length scale limitations. Further, differentiation is likely to involve some combination of mechanical and chemical processes. The main take home messages from these experiments should be: 1) that significant chemical differentiation of partially molten material will occur over cm scales on week time scales; 2) a fully connected compositionally changing melt can exist from 1,000 down to 350°C in a range of compositional systems. The demonstration that a plane of continuously changing silicate-carbonate liquids in equilibrium with nepheline in the phase equilibrium experiments provides a reason for the liquid continuum inferred in the nephelinite thermal migration experiments. The observation of systematic mineral layering and redistribution of elements in these experiments attests to the reactive and pervasive nature of the hydrous carbonate liquid which rapidly transports components by diffusion.

The observed capsule evolution from a partially-molten-everywhere initial condition to a nearly complete melt-crystal segregation is consistent with predicted thermal migration experiment behavior (Lesher and Walker, 1988). Furthermore, using IRIDIUM (Boudreau, 2003), which combines mineral-melt equilibrium calculations with diffusive transport equations, the

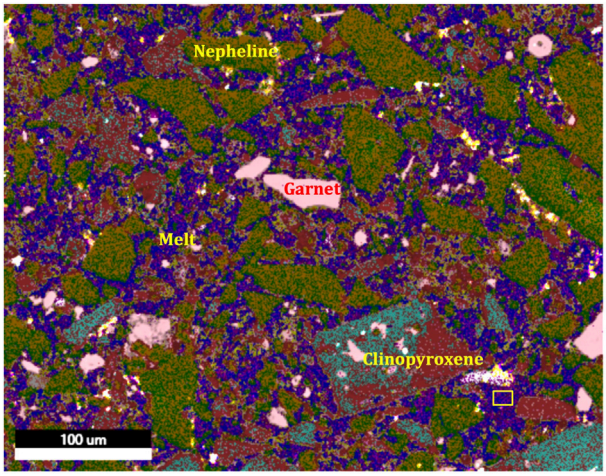

FIGURE 6
X-ray phase map of lower portion of ODL-5wk. Silicate minerals maintain their broken starting material appearance and are surrounded by quenched "melt" (deep blue in color) which based on EDS peaks consists of C-Na-Si-S-K-Ca-O (see text; yellow rectangle denotes location of analysis). Primary silicate minerals are nepheline (green), Ti-andradite garnet (pink), and clinopyroxene (turquoise and maroon). The grain labeled clinopyroxene shows how remnant high Mg CPX is replaced by NaFe clinopyroxene.

observed time evolution from ODL-2wk to ODL-5wk is reproduced (Supplementary Figure S4). This occurs despite the fact that the program does not include carbonate as a component in the melt and cannot calculate equilibria involving a melt below 600°C.

The systematic changes in mineral composition and mode with position (temperature) document that a continuous interconnected liquid must exist in the thermal migration experiments. The fact that no interface between two distinct (immiscible) liquids could be observed in any of these experiments argues for a continuum of liquid compositions from carbonate bearing nephelinite at high temperature (1,000°C) to a hydrous, alkalic carbonate (-silicate?) liquid at 350°C. Unfortunately, we must acknowledge that these experiments do not allow quantitative analyses of the interstitial liquid leaving compositions poorly known. However, the observed porosity (<3%) of plucked material along grain boundaries—which represents the maximum amount of liquid that could have existed—is clearly very small in each experiment. Indeed, most of ODL-5wk can be described as a "virtually melt (liquid)-free" crystal aggregate.

We infer that carbonate ion is a major constituent of the liquid everywhere and especially at lower temperatures based on the observation of increasing carbonate solids along silicate phase grain boundaries at the cold end of ODL-5wk. The x-ray tomograph (supplementary material movie) of ODL-1wk reveals rapid redistribution of U carbonates throughout the

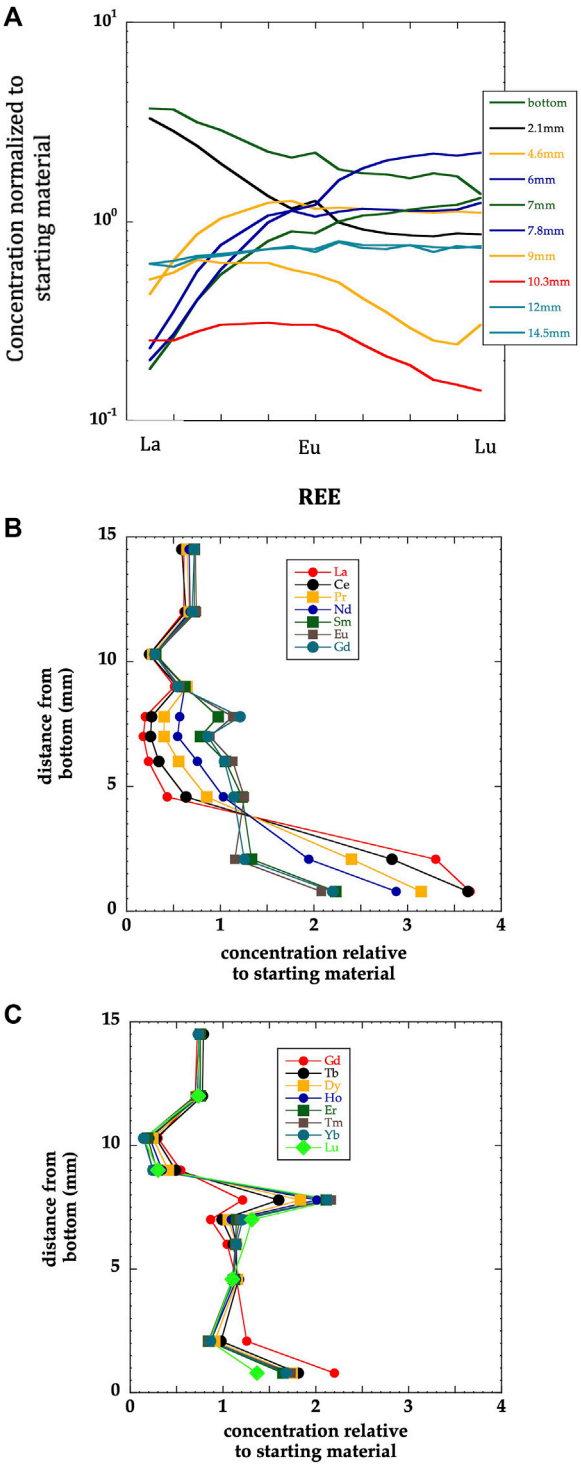

FIGURE 7
(A) normalized Rare Earth Element (REE) patterns change as a function of position, reflecting how REE partition between melt and the mineral assemblage at each temperature. For instance, the 7.8 mm pattern shows HREE enrichment due to garnet's presence, while the two bottom subsamples at the cold end of the experiment show LREE enriched patterns due to the presence of apatite and carbonates. The patterns are defined by analyses of
(Continued)

FIGURE 7 (Continued)
14 of the REE although element names on *x*-axis are omitted for readability. (B and C) Concentrations of LREE to MREE (normalized to starting material) and MREE to HREE as a function of position in the experiment. Note the systematic changes with z number across the range in REE with position in experiment: the strong and systematically low LREE in the 4.5–7.8 mm range corresponds to garnet and clinopyroxene combined. In the bottommost sample, note the systematic increase in concentration with decreasing z corresponding to carbonate and apatite control.

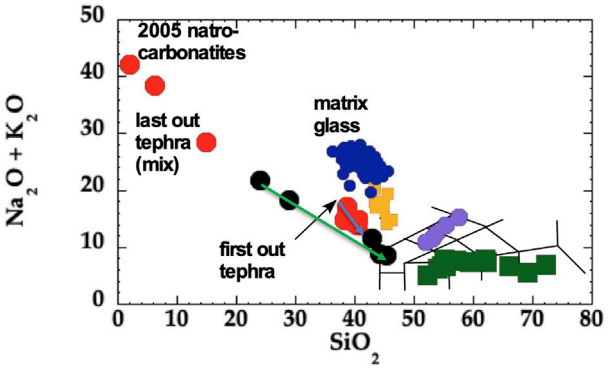

FIGURE 8
Total alkalis vs. silica (TAS) diagram expanded to full SiO_2 scale and to very high total alkali contents showing the observed trends in erupted ODL samples (red circles) and the ODL-5wk experiment (black circles). The first out tephra of the zoned nephelinite eruption of 2008 is marked with black arrow. Subsequently erupted less differentiated and more silicic samples trend down and to the right following the trend of the blue arrow. Note that the very last erupted tephra reflects a mix of carbonatite and nephelinite (thus is not representative of the decreasing silica differentiation trend). The two highest Na_2O+K_2O/lowest SiO_2 samples from ODL are the 2005 natrocarbonatite and 2007 tephra, show for reference. Sub-samples from the ODL-5wk experiment are shown as black circles. The lowest temperature sub-sample starts at $Na_2O+K_2O=22$ and sub-samples from progressively hotter levels in the experiment follow the green arrow trend. Thus, there is general correspondence of the down-temperature trend of differentiation observed in the ODL zoned eruption and the ODL-5wk experiment. Also shown are other ODL nephelinites (gold squares: Klaudius and Keller, 2006) and ODL 2008 matrix glasses (blue circles: de Moor et al., 2013). For reference, green squares are sub-samples from the Huang et al. (2009) thermal migration experiment involving wet andesite that reproduces Earth's calc-alkaline differentiation trends to silicic compositions. An alkalic differentiation trend is shown by the purple circles (data from the Masotta et al. (2011) thermal migration of phonolite experiment). Thus, igneous differentiation in the shallow crust could reflect a similar thermal gradient-based differentiation process operating on different compositions with total alkalis playing the decisive role in the trajectory of silica changes during differentiation.

capsule. Effectively, the carbonate minerals track the path of the liquid existing within these experiments. In addition, vertically aligned streaks of carbonates are observed running through nepheline grains, probably tracing the dissolution-reprecipitation pathway of the liquid directly through this mineral.

The un-Earth-like temperature gradients in thermal migration experiments may lead some to dismiss their relevance. However, comparison of the few studies to date presenting wet (H_2O bearing) thermal migration experiments with Earth's differentiation trends shows notable similarity in behavior on a TAS (total alkalis vs. silica) diagram (Figure 8). For instance, a study presenting an andesite plus 4 wt% H_2O experiment placed in a 950 to 350°C temperature offset produced a compositional trend of sub-samples that reproduces a calc-alkaline differentiation trend (Huang et al., 2009; also see AFM plot in Lundstrom, 2016). Likewise, a study of phonolite plus water with an 800–1,050°C temperature offset reproduces typical alkalic differentiation trends (Masotta et al., 2011). Here, ODL-5wk shows that thermal migration involving a hydrous nephelinite + Na_2CO_3 starting material produces an anti-correlated trend of subsamples in total alkalis against silica. Clearly, this is a unique compositional trend distinct from both calc-alkaline and alkalic trends with down temperature differentiation producing *lower* silica content materials.

Notably, the compositional evolution in ODL-5wk provides an intriguing parallel to the compositional zoning observed in the 2008 ODL eruption. On the TAS diagram, the 2008 eruption illustrates an endmember behavior whereby the down temperature differentiation trend leads toward increasing alkali contents, lower MgO and *decreasing* silica. Sub-samples of ODL-5wk mimic this trend with samples from the low temperature end having lower silica, lower MgO and higher alkali contents. Note that erupted ODL nephelinites are crystal-rich (like the bottom of the experiment), consistent with formation as a zoned crystal-rich mush that was then erupted. In other words, the differentiation trend on a TAS diagram reflects compositional changes of the whole crystal mush, not the evolution of the liquid alone.

It is well accepted that magma differentiation in natural samples conforms closely to the expectations of a process controlled by mineral-melt equilibrium. A hundred years of experimental petrology producing high quality phase equilibrium and partition coefficient data have built this as a foundation. Thus, there is agreement that the major and trace element trends of differentiation in Earth's magmatic systems follow predictions of mineral-melt equilibrium. However, how differentiation controlled by mineral-melt equilibrium actually works remains an open question. Despite sound arguments against crystal settling in mafic systems (Campbell, 1978; McBirney and Noyes, 1979), fractional crystallization involving mechanical separation of phases (as typically viewed) remains the paradigm for upper crustal differentiation of mafic magmas. The basis of support for this conclusion has been the ability to quantitatively model major and trace element changes by mass balance box models

(e.g., Gast, 1968). However, such models do not uniquely support a mechanical separation process—if diffusive transport timescales can keep up with vertical sill accumulation rates, a close approach to equilibrium phase behavior including trace element partitioning will occur. If so, a match between Gastian model and observation is simply not unique as the same mass balance-based box model would apply to this coupled diffusion-advection case. In summary, it is reasonable to ask if the diversity of igneous rocks, dominated by differentiation in the upper crust of the Earth, could reflect thermal migration processes and not fractional crystallization/crystal settling. While questions about transport scaling must always be considered, the notable similarity between trends of these experiments and the compositional trends observed for Earth's magmatic systems should give food for thought, given the observed paucity of large blobs of magma anywhere in Earth's upper crust.

Application to ODL: A strawman model for cyclicity and carbonatite formation

Igneous differentiation is most often attributed to mechanical separation of minerals from melt by fractional crystallization or partial melting. However, given the rapid diffusion of components observed in the thermal migration experiments, a thermal gradient-based differentiation process tied to sill emplacement may also be a viable mechanism for forming ODL's zoned magma body. The formation of hydrous carbonate-silicate liquid within a mineral mush leads to our suggested model (Figure 9) explaining three key features of ODL: 1) production of a nephelinite magma, "reversely" zoned in silica; 2) natrocarbonatite effusion; and 3) recurrence of eruption cycles.

We suggest ODL operates by continuous arrival and ponding of a CO_2-bearing nephelinitic melt to the upper crust, forming a sill complex which builds top down as arriving magmas pond beneath a permeability barrier in the volcanic pile. Such a scenario is consistent with high precision dating of many intrusions including granitic plutons which unambiguously build top down as sill complexes (Leuthold et al., 2012). When a sill emplaces, heat is preferentially lost out its upper contact. Younger sills underplate previous ones, heating the bottom of that sill, resulting in relatively strong thermal gradients. A constant rate of vertical sill accumulation balanced by steady vertical heat loss results in a moving thermal gradient zone where differentiation can occur building a compositionally zoned mush (Lundstrom, 2009). As a strawman example, imagine emplacement of sills approximately circular in shape in map view (~5 km in radius surrounding the volcano conduit). If the sills vertically accumulate at ~5 cm/yr for 30 years, the zoned mush (sill complex) would have a volume of ~5 x 10^7 m^3, approximately the volume of tephra erupted in 2008 (Kervyn et al., 2010). Vertical accumulation rates or sill complex aspect ratios could differ from this strawman but still give similar results. Regardless, simple heat flow calculations indicate that such thin sills in the upper crust will cool to <500°C quickly (Annen et al., 2006). Yet the arrival of new sills maintains the high temperature end of the gradient, providing an imposed thermal gradient on the differentiating mush.

Compositional differentiation would thus follow trends dictated by mineral-melt equilibrium as long as the Peclet number (the relative length scales of vertical accumulation of sills vs. mass diffusion: LV/D) is ~1. Given 5 cm of sill accumulation in a year and a diffusivity of 10^{-5} cm^2/s, thermal gradient differentiation will operate over a ~0.6 m effective length scale, thus satisfying the Peclet requirement. Thus, we suggest this top-down sill complex builds a nephelinite mush with its cooler top having lower SiO_2 and MgO and its hotter bottom having the opposite.

The finding that a hydrous carbonate liquid forms at the cold end of thermal migration experiments explains the second feature of this model. Adding a twist to the top-down sill differentiation model of Lundstrom (2009), we suggest this low viscosity liquid will be buoyant relative to the minerals in the mush. Viscosities are likely <10^{-3} Pas based on measurements of Na_2CO_3 (Dobson et al., 1996; Stagno et al., 2018) and hydrous Na-silicates (Yang et al., 2008). Thus, this liquid will form and percolate up through the mush and eventually ooze out the surface, erupted as natrocarbonatite. During its final ascent through the crust, it will degas H_2O at near surface pressure, emanating as the dry natrocarbonatite lava at ~450–500°C as observed. Such a model presents a significant advance on both the fluid condensate (Nielsen and Veksler, 2002) and liquid immiscibility (Freestone and Hamilton, 1980; ChurchJones, 1995; Kjarsgaard et al., 1995; Mitchell, 2009) models for natrocarbonatite formation by producing a carbonate liquid without invoking formation of a second liquid/vapor phase. Our experiments document a plausible liquid at ~400°C, similar to natrocarbonatite eruption temperatures; in contrast, the liquid immiscibility model requires hundreds of degrees of further cooling and differentiation, despite no evidence for it. Indeed, given our experiments which show no sharp carbonate-silicate melt immiscibility boundary anywhere, it can be questioned whether immiscibility would occur in the realistic scenario of a crustal thermal gradient. Finally, a similar upflow of hydrous low temperature silicate liquids up through mush zones has recently been proposed as a major process occurring in granitic plutons (Lundstrom et al., 2022)—an implication of upward advection of these water-rich liquids is that they will rapidly remove heat from magma systems, strongly

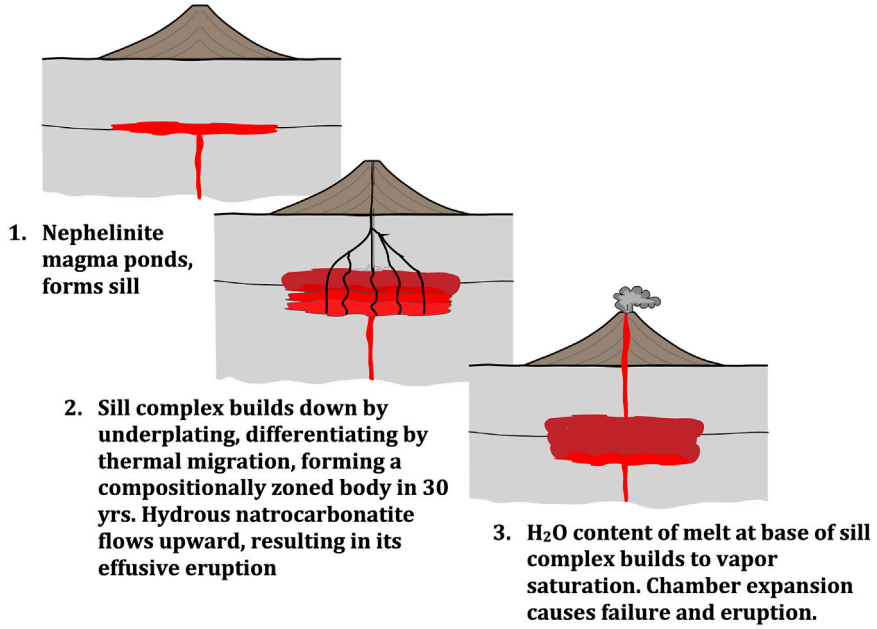

FIGURE 9
Cartoon depicting stages in the temporal evolution and ~30 years eruption cycles of Ol Doinyo Lengai volcano. In stage 1, nephelinite magmas begin to pond in the upper crust after encountering a permeability barrier. Next, sills build down with time forming a moving temperature gradient zone that forms a compositionally zoned mush body. During this time, H_2O-Na_2CO_3 liquid ascends through the mush and effusively erupts—degassing of H_2O from this liquid at low pressure results in the anhydrous natrocarbonatite observed. Finally, as this sill complex grows top down, H_2O dissolved in silicate melt builds up in the nephelinite that occurs at the arriving sill/base of the system. At ODL, the rise in melt H_2O content occurs over a 30 years time scale, ultimately resulting in H_2O vapor saturation that drives explosive eruption of the silicate magma by carapace failure (vertical scale of sill complex is exaggerated for clarity). Vertical scale approximate (sill thickness exaggerated and depth of sill complex is not specified).

influencing isotherms and shortening the thickness of the thermal gradient differentiation zone. If hydrous alkalic liquids commonly flow up through and above sill complexes, it would have profound impact on models of differentiation on Earth.

The third feature of this model is that it may explain the cyclical eruption behavior of ODL. We posit that H_2O will build up in the liquid layer at the base of the sill complex over the 30 years repose interval of ODL. H_2O vapor saturation in this liquid ultimately causes the explosive silicate eruption. As the experiment illustrates, H_2O concentrations must increase in the melt-rich layer at the base of the sill complex as it builds down because the mush consists of anhydrous minerals. We can use the observed H_2O behavior in ODL-5wk to constrain the partitioning of H_2O between melt and mush: the experiment starts with 2 wt% H_2O homogeneously distributed and evolves to a melt in the upper 25% of the capsule having 3 wt% H_2O. If so, H_2O in the area of arriving melt at the base of the sill complex would reach ~9.6 wt% H_2O in ~30 years (assuming ODL nephelinites start with 2 wt% H_2O). This concentration is similar to H_2O measured in nepheline melt inclusions in the 2008 eruption (de Moor et al., 2013). We suggest that when H_2O vapor saturation occurs, the chamber undergoes expansion and carapace cracking, causing depressurization, devolatilization and finally catastrophic eruption of zoned silicate mush (Gregg et al., 2012). Thus, this model provides a plausible mechanism for eruption triggering over a fixed but short timescale, with repose interval between eruptions directly tied to the amount of magma added.

This model explains several important geochemical features of ODL. First, large fractionations of very short-lived parent-daughter pairs within the U-series decay chain occur. For instance (^{228}Ra)/(^{232}Th) are >5 in a 1988 natrocarbonatite (Pyle et al., 1991) indicating Ra-Th fractionation <10 years before eruption. If this fractionation reflects two immiscible melts separating, full separation must occur in 10 years (or possibly even less)—while this may be possible, the strict timing does raise questions to this model. In contrast, using our upflow model, Th-Ra fractionation could literally occur just prior to emanation from the ground through simple partitioning or even sorption like processes. Second, experiments measuring trace element partitioning between two immiscible melts poorly match trace element patterns of ODL natrocarbonatite (Nielsen and Veksler, 2002). Although a pure carbonatite melt cannot be analyzed in these experiments, we can compare bulk element concentrations between the bottom of the capsule (dominated by hydrous carbonate melt) and the nephelinite material at higher

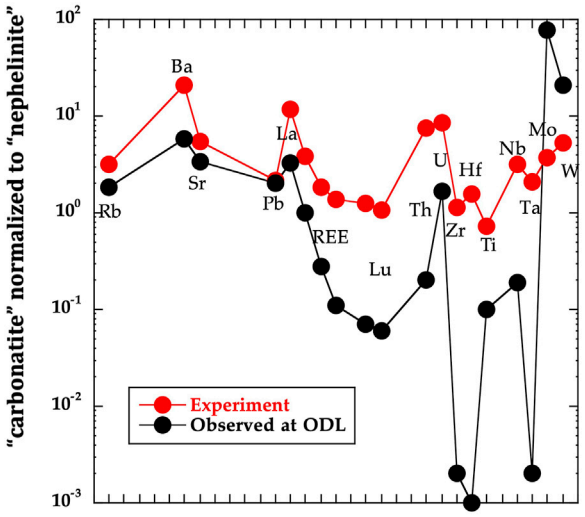

FIGURE 10
Ratio of "natrocarbonatite concentrations" to "nephelinite concentrations" for the spidergram of trace elements given. For "observed at ODL" we have used the 2005 natrocarbonatite and 2008 ODL-5 nephelinite. In the case of the ODL-5wk experiment, we have take sub-sample concentration average of the lower two sub-samples divided by the average of the upper six subsamples (nephelinite mush). A general similarity of behavior is evident based on the pattern reproduction. Certain high field strength elements poorly match, reflecting the fact that abundant clinopyroxene and garnet (which hold these elements) still exist within this "natrocarbonatite" sub-sample (see text).

temperature (averaging ablation transects). This relative comparison shows strong enrichments in LREE, Th, U, W and Mo of the carbonate material relative to the nephelinite material. The trace element pattern made by comparison of the two parts of the experiment provides qualitative reproduction of the pattern of ODL natrocarbonatite compared to nephelinite (Figure 10). In detail, both clinopyroxene and garnet are still present and thus included in the bulk concentrations of the carbonate-rich sample (at bottom of experiment). This probably greatly increases Ti, Zr, Hf, Ta and Th concentrations in the experimental "carbonatite", perhaps accounting for the relative mismatch of these elements. Notably, the shape of the REE patterns for the two bottom-most samples of the ODL-5wk (Figure 7) matches those of ODL natrocarbonatite with relatively flat MREE to HREE slopes but steep slopes on the LREE. Thus, a model of natrocarbonatite melt percolating up through nephelinite mush likely could produce trace element patterns similar to those observed in ODL natrocarbonatites.

Application of the model to syenites and alkali ring complexes

Alkali ring-complexes involving ubiquitous alkali metasomatism surround carbonatite dikes (feeder zones) throughout the world. Magnet Cove, Arkansas, provides an excellent example reflecting an alkalic ring of syenites of ~5 km radius around an intrusive core of spar calcite (Erickson and Blade, 1963; Flohr and Ross, 1990). While the calcitic core is interpreted to reflect crystallization of calcium carbonate magma, precipitation of calcite from an ODL-like sodium carbonatite liquid is equally plausible. Indeed, recent work on an ancient calcio-carbonatite from Canada found that calcite crystals contain abundant Na_2CO_3 fluid inclusions (Chen and KamenetskySimonetti, 2013). This raises the possibility that some calcio-carbonatites found around the world could reflect calcite crystallization from ODL-like hydrous natrocarbonatite liquids. The sodic nature of natrocarbonatite provides a ready explanation for the extensive alkali metasomatism that ubiquitously occurs around carbonatite complexes such as Magnet Cove.

Magnet Cove consists of a calcite core surrounded by concentric layers of ijolite (nepheline, clinopyroxene, melilite garnet) and various syenites (pseudoleucite, sphene; Erickson and Blade, 1963). The Magnet Cove ijolite is very similar compositionally to ODL nephelinites having 41 wt% SiO_2 and 3 wt% MgO. Outward from the calcite/ijolite core, the syenites become progressively more differentiated with MgO reaching values as low as 0.2 wt%. Other indexes of differentiation such as FeO, CaO, TiO_2 and P_2O_5 also systematically decrease away from the core of the complex (Flohr and Ross, 1990). Thus, the ring sequence follows down temperature evolution consistent with the outermost portions being cooled by contact with ambient crust. A final connection between experiment and syenite formation is the compositional similarity between glass inclusions in Tenerife syenites (Wolff and Toney, 1993) and the liquids determined here in equilibrium with albite and nepheline.

Carbonate-water-silicate interactions control volatile solubility in alkalic systems

We have provided two lines of evidence supporting our inference that a continuum of liquid compositions co-exists in equilibrium with nepheline as temperature decreases, changing from a hydrous alkali silicate melt with dissolved carbonate to a hydrous carbonate-silicate liquid at lower temperature. First, the systematic compositional change and mineralogical layering from 1,000 to 350°C in thermal migration experiments could not occur unless a fully connected liquid existed. Second, liquid compositions in isothermal crystallization experiments evolve down temperature in a manner consistent with previous work (Schairer and Bowen, 1947) and only show existence of liquid (glass) at <500°C when carbonate was added to the system. While there is a bit of disconnect between the feldspar saturated simple system experiments and the more complicated nephelinite thermal migration runs where feldspar was usually not present (it was present in ODL-1wk due to Ba addition), inferring a hydrous-carbonate-silicate continuum is not an over-interpretation.

The miscibility between carbonate and silicate might be fully expected based both on melt polymerization and compositional changes with temperature. For instance, as temperature decreases and less aluminum is incorporated into the melt, it is expected that water solubility into the melt will increase (Mysen et al., 2000). The solubility of Na_2CO_3 into a hydrous Na silicate liquid might also be expected based on the completely depolymerized structure of both liquids. For instance, spectroscopic studies have found silica dimers to be the most common structure in hydrous Na silicate liquids (Svensson et al., 1986). Finally, with the demonstrated existence of a continuum of liquids existing from 1,000 down to 350°C in the thermal gradient experiments, the known small wetting angles of carbonate fluids (WatsonBrenan, 1987; Hunter and McKenzie, 1989) explains the profound observation that a large amount of differentiation occurs with virtually no observable liquid present. Lastly, the silicate to carbonate melt continuum also would have profound implications for mobilization of REE and critical mineral deposits.

Production of carbonatite as a down temperature differentiation product of basalt is consistent with previous conclusions (FischerBurnard et al., 2012) that ODL natrocarbonatite does not form from a strongly CO_2 enriched source but instead reflects derivation from typical alkali basalt. For instance, if the ODL parent magma had a CO_2/Nb of 100 (FischerBurnard et al., 2012) and 250 ppm Nb (typical East Africa Rift alkali basalt), it would not be vapor saturated upon arrival in the upper crust. In other words, a fairly typical enriched mantle alkalic basalt can account for the CO_2 forming the natrocarbonatites. What appears to be unusual about ODL is its Na_2O content and this appears to control how the volcano releases its CO_2.

Volcanic outputs of CO_2 gas represent a significant atmospheric input that play a major role in Earth's carbon cycle over 10^4–10^5 year timescales with rifts playing a major role in release of CO_2 sequestered in the continental lithosphere (Brantley and Koepenick, 1995; Brune et al., 2017). Yet why certain volcanoes output more CO_2 remains nebulous. For instance, while the ODL system is obviously extremely rich in oxidized carbon, its CO_2 degassing flux is much smaller than another alkalic volcano on the western East Africa Rift, Nyiragongo (Burton et al., 2013; Foley and Fischer, 2017).

Comparison of bulk compositions of erupted nephelinites from ODL and Nyiragongo show that ODL nephelinites have upwards of 11 wt% Na_2O (along with ~2 wt% CO_2) while nephelinites at Nyiragongo are much less sodic (~5 wt%; Andersen et al., 2012; Sawyer et al., 2008). We suggest the Nyiragongo system is unlikely to form the hydrous Na-carbonate-silicate liquid that ODL forms (due to its lower Na_2O), thus a CO_2 vapor forms and outgases. Water contents for Nyiragongo are unknown but may also play an important role in stabilization of these liquids. Thus, ODL, with much greater total CO_2 content, ironically results in less delivery of CO_2 to the atmosphere because of its more alkalic nature.

Conclusion

Results of isothermal crystallization and thermal gradient experiments provide documentation that in alkalic systems a continuously changing liquid composition in equilibrium with nepheline exists from 1,000°C down to 350°C. This liquid continuum reflects nephelinites containing 4 wt% CO_2 at high temperature evolving to hydrous carbonate silicate liquids at low temperature. This study is only a start to understanding the possibility of low temperature liquids in peralkaline silica-undersaturated systems and full assessment of their impact is yet to come. Clearly more work determining the compositions of these liquids is needed for a fuller understanding of mineral saturation and reaction. These results are applied to Ol Doinyo Lengai, a volcano known for cycles of quiescent natrocarbonatite punctuated by explosive eruptions every 30 years. A model of arriving nephelinite magmas forming a sill complex explains: 1) the production of natrocarbonatite, 2) the unusual zoning of erupted nephelinite, and 3) the 30 yr. cycles of eruption at ODL. The high Na_2O contents of ODL magmas allow a hydrous Na_2CO_3 melt to be stabilized at low temperatures, limiting the amount of CO_2 degassing at ODL. In contrast, Nyiragongo magmas have much lower Na_2O leading to a much higher CO_2 degassing flux than ODL.

The experiments illustrate that a remarkable amount of differentiation can occur within a solid material having virtually no observable melt, probably reflecting the presence of carbonate-rich liquid with its known wetting behavior. This could explain the contradiction between the dearth of melt bodies observed by seismology in the upper crust and the corresponding high electrical conductivity seen in the same areas of crust. The results presented here show that a carbonate-bearing liquid can efficiently wet the surfaces of crystals, providing a pathway for rapid movement of liquid even when total melt porosity is low. As a result of the fast reaction and transport properties of this liquid, magmas can remain in local equilibrium with crystals (nepheline and pyroxene in this case) allowing trace element fractionations related to chemical exchange to occur over scales ranging from cm to meters with application to kilometer scales if coupled to realistic physical models.

Data availability statement

The original contributions presented in the study are included in the article/Supplementary Material, further inquiries can be directed to the corresponding author.

Author contributions

CL, XL, RG-D, and ZZ performed experiments and x-ray analyses, RH performed SIMS analyses, MS and LY performed tomography analyses, TF contributed samples and performed volatile analyses. All authors contributed to writing.

Funding

This work was funded under NSF EAR 14-27386.

Acknowledgments

We thank two reviewers for helpful comments that greatly improved the work. Comments from editor JW were especially useful. We hope the ideas here will spur further work on the role of low temperature (igneous) liquids in Earth's crust and mantle.

Conflict of interest

The authors declare that the research was conducted in the absence of any commercial or financial relationships that could be construed as a potential conflict of interest.

Publisher's note

All claims expressed in this article are solely those of the authors and do not necessarily represent those of their affiliated organizations, or those of the publisher, the editors and the reviewers. Any product that may be evaluated in this article, or claim that may be made by its manufacturer, is not guaranteed or endorsed by the publisher.

Supplementary material

The Supplementary Material for this article can be found online at: https://www.frontiersin.org/articles/10.3389/feart.2022.970264/full#supplementary-material

References

Ackerson, M. R., Mysen, B. O., Talby, N. D., and Watson, E. B. (2018). Low-temperature crystallization of granites and the implications for crustal magmatism. *Nature* 559, 94–97. doi:10.1038/s41586-018-0264-2

Andersen, N. L., Jicha, B. R., Singer, B. S., and Hildreth, W. (2017). Incremental heating of Bishop Tuff sanidine reveals preeruptive radiogenic Ar and rapid remobilization from cold storage. *PNAS* 114, 12407–12412. doi:10.1073/pnas.1709581114

Andersen, T., Elburg, M., and Erambert, M. (2012). Petrology of combeite- and götzenite-bearing nephelinite at Nyiragongo, virunga volcanic province in the East African Rift. *Lithos* 152, 105–121. doi:10.1016/j.lithos.2012.04.018

Annen, C., Scaillet, B., and Sparks, R. S. J. (2006). Thermal constraints on the emplacement rate of a large intrusive complex: The manaslu leucogranite, Nepal himalaya. *J. Petrology* 47, 71–95. doi:10.1093/petrology/egi068

Boudreau, A. E. (2003). IRIDIUM; a program to model reaction of silicate liquid infiltrating a porous solid assemblage. *Comput. Geosciences* 29, 423–429. doi:10.1016/s0098-3004(02)00119-x

Brantley, S. L., and Koepenick, K. W. (1995). Measured carbon dioxide emissions from Oldoinyo Lengai and the skewed distribution of passive volcanic fluxes. *Geol.* 23, 933. doi:10.1130/0091-7613(1995)023<0933:mcdefo>2.3.co;2

Brune, S., Williams, S. E., and Müller, R. D. (2017). Potential links between continental rifting, CO_2 degassing and climate change through time. *Nat. Geosci.* 10, 941–946. doi:10.1038/s41561-017-0003-6

Burton, M. R., Sawyer, G. M., and Granieri, D. (2013). Deep carbon emissions from volcanoes. *Rev. Mineral. Geochem.* 75, 323–354. doi:10.2138/rmg.2013.75.11

Campbell, I. H. (1978). Some problems with the cumulus theory. *Lithos* 11, 311–323. doi:10.1016/0024-4937(78)90038-5

Chen, W., Kamenetsky, V. M., and Simonetti, A. (2013). Evidence for the alkaline nature of parental carbonatite melts at Oka complex in Canada. *Nat. Commun.* 4, 2687. doi:10.1038/ncomms3687

Church, A. A., and Jones, A. P. (1995). Silicate-carbonate immiscibility at oldoinyo Lengai. *J. Petrology* 36, 869–889. doi:10.1093/petrology/36.4.869

Davis, J. W., Coleman, D. S., Gracely, J. T., Gaschnig, R., and Stearns, M. (2012). Magma accumulation rates and thermal histories of plutons of the Sierra Nevada batholith, CA. *Contrib. Mineral. Pet.* 163, 449–465. doi:10.1007/s00410-011-0683-7

Dawson, J. B., Keller, J., and Nyamweru, C. (1995). "Historic and recent eruptive activity of oldoinyo Lengai," in *Carbonatite volcanism: Oldoinyo Lengai and the petrogenesis of natrocarbonatites*. Editors K. Bell and Jörg Keller (Berlin, Heidelberg: Springer Berlin Heidelberg), 4–22. doi:10.1007/978-3-642-79182-6_2

Dawson, J. B. (1962). The geology of Ol Doinyo Lengai. *Bull. Volcanol.* 24, 349–387. doi:10.1007/bf02599356

de Moor, J. M., Fischer, T. P., King, P. L., Botcharnikov, R. E., Hervig, R. L., Hilton, D. R., et al. (2013). Volatile-rich silicate melts from Oldoinyo Lengai Volcano (Tanzania); implications for carbonatite Genesis and eruptive behavior. *Earth Planet. Sci. Lett.* 361, 379–390. doi:10.1016/j.epsl.2012.11.006

Dobson, D., Jones, A., Richard, R., Sekine, T., Kurita, K., Taniguchi, T., et al. (1996). *In-situ* measurement of viscosity and density of carbonate melts at high pressure. *Earth Planet. Sci. Lett.* 143, 207–215. doi:10.1016/0012-821x(96)00139-2

Edgar, A. D. (1964). Phase-equilibrium relations in the system nepheline-albite-water at 1, 000 Kg/cm2. *J. Geol.* 72, 448–460. doi:10.1086/627001

Erickson, R. L., and Blade, L. V. (1963). Geochemistry and petrology of the alkalic igneous complex at Magnet Cove, Arkansas. Professional Paper. *U. S. Geol. Surv.* 425, 1–95. doi:10.3133/pp425

Fischer, T. P., Burnard, P., Marty, B., Hilton, D. R., Fu, E. F., Palhol Sharp, Z. D., et al. (2012). Upper-mantle volatile chemistry at Oldoinyo Lengai volcano and the origin of carbonatites. *Nature* 459, 77–80. doi:10.1038/nature07977

Flohr, M. J. K., and Ross, M. (1990). Alkaline igneous rocks of Magnet Cove, Arkansas: Mineralogy and geochemistry of syenites. *Lithos* 26, 67–98. doi:10.1016/0024-4937(90)90041-x

Foley, S. F., and Fischer, T. P. (2017). An essential role for continental rifts and lithosphere in the deep carbon cycle. *Nat. Geosci.* 10, 897–902. doi:10.1038/s41561-017-0002-7

Freestone, I. C., and Hamilton, D. L. (1980). The role of liquid immiscibility in the Genesis of carbonatites-an experimental study. *Contr. Mineral. Pet.* 73, 105–117. doi:10.1007/bf00371385

Gaillard, F., Malki, M., Iacono-Marziano, G., Pichavant, M., and Scaillet, B. (2008). Carbonatite melts and electrical conductivity in the asthenosphere. *Science* 322, 1363–1365. doi:10.1126/science.1164446

Gast, P. W. (1968). Trace element fractionation and the origin of tholeiitic and alkaline magma types. *Geochim. Cosmochim. Acta* 32, 1057–1086. doi:10.1016/0016-7037(68)90108-7

Gregg, P. M., de Silva, S. L., Grosfils, E. M., and Parmigiani, E. (2012). Catastrophic caldera- forming eruptions: Thermomechanics and implications for eruption triggering and maximum caldera dimensions on Earth. *J. Volcanol. Geotherm. Res.* 241-242, 1–12. doi:10.1016/j.jvolgeores.2012.06.009

Hamilton, D. L., and MacKenzie, W. S. (1965). Phase-equilibrium studies in the system $NaAlSiO_4$ (nepheline)–$KAlSiO_4$ (kalsilite)–SiO_2-H_2O. *Mineral. Mag. J. Mineral. Soc.* 34, 214–231. doi:10.1180/minmag.1965.034.268.17

Hill, G. J., Caldwell, T. G., Heise, W., Chertkoff, D. G., Bibby, H. M., Burgess, M. K., et al. (2009). Distribution of melt beneath mount St helens and mount Adams inferred from magnetotelluric data. *Nat. Geosci.* 2, 785–789. doi:10.1038/ngeo661

Huang, F., Lundstrom, C. C., Glessner, J., Ianno, A., Boudreau, A., Li, J., et al. (2009). Chemical and isotopic fractionation of wet andesite in a temperature gradient: Experiments and models suggesting a new mechanism of magma differentiation. *Geochim. Cosmochim. Acta* 73, 729–749. doi:10.1016/j.gca.2008.11.012

Hunter, R. F., and McKenzie, D. (1989). The equilibrium geometry of carbonate melts in rocks of mantle composition. *Earth Planet. Sci. Lett.* 92, 347–356. doi:10.1016/0012-821x(89)90059-9

Jones, A. P., Genge, M., and Carmody, L. (2013). Carbonate melts and carbonatites. *Rev. Mineral. Geochem.* 75, 289–322. doi:10.2138/rmg.2013.75.10

Kamentesky, V. S., Doroshkevich, A. G., Elliott, H. A. L., and Zaitsev, A. L. (2021). Carbonatites: Contrasting, complex, and controversial. *Elements* 17, 307–314. doi:10.2138/gselements.17.5.307

Kervyn, M., Ernst, G. J. G., Keller, J., Vaughan, R. G., Klaudius, J., Pradal, E., et al. (2010). Fundamental changes in the activity of the natrocarbonatite volcano oldoinyo Lengai, Tanzania: II. Eruptive behaviour during the 2007–2008 explosive eruptions. *Bull. Volcanol.* 72, 913–931. doi:10.1007/s00445-010-0360-0

Kjarsgaard, B., Hamilton, D., and Peterson, T. (1995). "Peralkaline nephelinite/carbonatite liquid immiscibility: Comparison of phase compositions in experiments and natural lavas from oldoinyo Lengai," in *Carbonatite volcanism: Oldoinyo Lengai and the petrogenesis of natrocarbonatites*. Editors K. Bell and J. Keller (Berlin: Springer), 219.

Koster van Groos, A. F. (1990). High-pressure DTA study of the upper three-phase region in the system Na_2CO_3-H_2O. *Amer. Mineral.* 75, 667–675.

Lees, J. M. (1992). The magma system of mount St. Helens: Non-linear high resolution P-wave tomography. *J. Volcanol. Geotherm. Res.* 53 (1–4), 103–116. doi:10.1016/0377-0273(92)90077-q

Lesher, C. E., and Walker, D. (1988). Cumulate maturation and melt migration in a temperature gradient. *J. Geophys. Res.* 93, 10295–10311. doi:10.1029/jb093ib09p10295

Leuthold, J., Müntener, O., Baumgartner, L. P., Putlitz, B., Ovtcharova, M., and Schaltegger, U. (2012). Time resolved construction of a bimodal laccolith (Torres del Paine, Patagonia). *Earth Planet. Sci. Lett.* 325, 85–92. doi:10.1016/j.epsl.2012.01.032

Liu, Y. S., Hu, Z. C., Gao, S., Guenther, D., Xu, J., Gao, C. G., et al. (2008). *In situ* analysis of major and trace elements of anhydrous minerals by LA-ICP-MS without applying an internal standard. *Chem. Geol.* 257, 34–43. doi:10.1016/j.chemgeo.2008.08.004

Lowenstern, J. (2001). Carbon dioxide in magmas and implications for hydrothermal systems. *Miner. Deposita* 36, 490–502. doi:10.1007/s001260100185

Lundstrom, C. C. (2020). Continuously changing quartz-albite saturated melt compositions to 330°C with application to heat flow and geochemistry of the ocean crust. *J. Geophys. Res. Solid Earth* 125. doi:10.1029/2019JB017654

Lundstrom, C. C. (2009). Hypothesis for the origin of convergent margin granitoids and Earth's continental crust by thermal migration zone refining. *Geochim. Cosmochim. Acta* 73, 5709–5729. doi:10.1016/j.gca.2009.06.020

Lundstrom, C. C., Lin, X., Brueckel, K., Campe, C., Nan, X., Ortega, K., et al. (2022). A new mechanism for forming thick granitic continental crust at phanerozoic convergent margins. *GSA Books. Hamilt.* 553, 233–249. in press volume. doi:10.1130/2021.2553(20)

Lundstrom, C. C. (2016). The role of thermal migration and low temperature melt in granitoid formation: Can granites form without rhyolite melt? *Int. Geol. Rev.* 58, 371–388. doi:10.1080/00206814.2015.1092098

Masotta, M., Freda, C., and Gaeta, M. (2011). Origin of crystal-poor, differentiated magmas: Insights from thermal gradient experiments. *Contrib. Mineral. Pet.* 163, 49–65. doi:10.1007/s00410-011-0658-8

McBirney, A. R., and Noyes, R. M. (1979). Crystallization and layering of the skaergaard intrusion. *J. Petrology* 20, 487–554. doi:10.1093/petrology/20.3.487

Mitchell, R. (2009). Peralkaline nephelinite–natrocarbonatite immiscibility and carbonatite assimilation at Oldoinyo Lengai, Tanzania. *Contrib. Mineral. Pet.* 158, 589–598. doi:10.1007/s00410-009-0398-1

Moussallam, Y., Morizet, Y., and Gaillard, F. (2016). H_2O–CO_2 solubility in low SiO_2-melts and the unique mode of kimberlite degassing and emplacement. *Earth Planet. Sci. Lett.* 447, 151–160. doi:10.1016/j.epsl.2016.04.037

Mysen, B. O., and Wheeler, K. (2000). Solubility behavior of water in haploandesitic melts at high pressure and high temperature. *Am. Mineralogist* 85, 1128–1142. doi:10.2138/am-2000-8-903

Nielsen, T. F., and Veksler, I. V. (2002). Is natrocarbonatite a cognate fluid condensate? *Contrib. Mineral. Pet.* 142, 425–435. doi:10.1007/s004100100306

Pan, D., and Galli, G. (2016). The fate of carbon dioxide in water-rich fluids under extreme conditions. *Sci. Adv.* 2, e1601278. doi:10.1126/sciadv.1601278

Pyle, D. M., Dawson, J. B., and Ivanovich, M. (1991). Short-lived decay series disequilibria in the natrocarbonatite lavas of oldoinyo Lengai, Tanzania: Constraints on the timing of magma Genesis. *Earth Planet. Sci. Lett.* 105, 378–396. doi:10.1016/0012-821x(91)90179-l

Reynes, J., Lanari, P., and Hermann, J. (2020). A mapping approach for the investigation of Ti–OH relationships in metamorphic garnet. *Contrib. Mineral. Pet.* 175, 46. doi:10.1007/s00410-020-01681-5

Rubin, A. E., Cooper, K. M., Till, C. B., Kent, A. J., Costa, F., Bose, M., et al. (2017). Rapid cooling and cold storage in a silicic magma reservoir recorded in individual crystals. *Science* 356, 1154–1156. doi:10.1126/science.aam8720

Sawyer, G. M., Carn, S. A., Tsanev, V. I., Oppenheimer, C., and Burton, M. (2008). Investigation into magma degassing at Nyiragongo volcano, democratic republic of the Congo. *Geochem. Geophys. Geosyst.* 9. doi:10.1029/2007GC001829

Schairer, J. F., and Bowen, N. L. (1947). Melting relations in the systems Na 2 O-Al 2 O 3 -SiO 2 and K 2 O-Al 2 O 3 -SiO 2. *Am. J. Sci.* 245, 193–204. doi:10.2475/ajs.245.4.193

Schairer, J. F., and Bowen, N. L. (1956). The system Na2O-Al2O3-SiO2. *Am. J. Sci.* 251, 129–195. doi:10.2475/ajs.254.3.129

Stagno, V., Stopponi, V., Kono, Y., Manning, C. E., and Irifune, T. (2018). Experimental determination of the viscosity of Na2CO3 melt between 1.7 and 4.6 GPa at 1200–1700 °C: Implications for the rheology of carbonatite magmas in the Earth's upper mantle. *Chem. Geol.* 501, 19–25. doi:10.1016/j.chemgeo.2018.09.036

Svensson, I. L., Sjoberg, S., and Ohman, L. O. (1986). Polysilicate equilibria in ConcentratedSodium silicate solutions. *J. Chem. Soc. Faraday Trans.* 82 (1), 3635–4364. doi:10.1039/f19868203635

Tuttle, O. F., and Bowen, N. L. (1958). Origin of granite in light of experimental studies in the system $NaAlSi_3O_8$-$KAlSi_3O_8$- SiO_2-H_2O. *Geol. Soc. Am. Mem.* 74, 1–145. doi:10.1130/MEM74

Watson, E. B., and Brenan, J. M. (1987). Fluids in the lithosphere, 1. Experimentally-determined wetting characteristics of CO2H2O fluids and their implications for fluid transport, host-rock physical properties, and fluid inclusion formation. *Earth Planet. Sci. Lett.* 85, 497. doi:10.1016/0012-821X(87)90144-0

Wolff, J. A., and Toney, J. B. (1993). Trapped liquid from a nepheline syenite: A re-evaluation of Na-Zr-F-rich interstitial glass in a xenolith from Tenerife, canary islands. *Lithos* 29, 285–293. doi:10.1016/0024-4937(93)90022-5

Woolley, A. R., and Church, A. A. (2005). Extrusive carbonatites: A brief review. *Lithos* 85, 1–14. doi:10.1016/j.lithos.2005.03.018

Yang, X., Zhu, W., and Yang, Q. (2008). The viscosity properties of sodium silicate solutions. *J. Solut. Chem.* 37, 73–83. doi:10.1007/s10953-007-9214-6